

COMPACTIFICATIONS OF PHYLOGENETIC SYSTEMS AND ELECTRICAL NETWORKS

SATYAN L. DEVADOSS AND STEFAN FORCEY

ABSTRACT. We demonstrate a graphical map, a new correspondence between circular electrical networks and circular planar split systems. When restricted to the *planar* circular electrical case, this graphical map finds the split system associated uniquely to the Kalmanson resistance distance of the dual network, matching the induced split system familiar from phylogenetics. This is extended to compactifications of the respective spaces, taking cactus networks to the newly defined compactified split systems. The graphical map preserves both components and cactus structure, allowing an elegant enumeration of induced phylogenetic split systems.

1. INTRODUCTION

At first glance the scientific pursuits of phylogenetics and circuit design seem to have little in common. In one we seek to uncover ancestral connections in a mysterious past, in the other to build electrical connections that achieve a desired effect. However, in both cases we are trying to find a structure—a mathematical network—which fits a known list of parameters. The resistance matrix for a circular planar electrical network turns out to be identical to a specialized phylogenetic distance matrix. Thus methods from phylogenetics are immediately useful for circular planar electrical networks.

We leverage several tools for the study of networks that are usually seen in differing contexts: Kron reduction and circular minors on the one hand, split networks on the other. The former is named for Gabriel Kron, who is responsible for much of the early work connecting electrical circuits, linear algebra, and graph theory. The Kron reduction [12] refers to a replacement of a circular electrical network with a less interconnected version which is indistinguishable from the original, from the point of view of its terminal, or boundary, nodes. The response matrix of the original is indeed the Laplacian of the Kron reduced network.

Spaces of *circular electrical networks* have been studied thoroughly over the last couple of decades. Collected early results are in the book by Curtis and Morrow [7]. More recently, the state of the art for circular planar electrical networks is represented by Kenyon and Wilson [28, 29, 30], Kenyon and Hersh [25], and Gao, Lam, and Xu [24]. The space of circular *planar* electrical networks is an embedded slice of the totally nonnegative Grassmannian, and thus projected into the *amplituhedron*, as shown in several papers by Galashin, Karp, and Lam [17, 18, 19, 20, 33]. Connections to planar graphs (which represent classes of directed networks) have been made by Galashin, Postnikov, and Williams [21]. Recognizing the planarity of a network and recovering its conductances both saw improvements in efficiency [1, 30].

2000 *Mathematics Subject Classification.* 05C50, 05C10, 92D15, 94C15, 90C05, 52B11.

Key words and phrases. phylogenetic networks, electrical networks, metrics, splits, polytopes.

Spaces of *circular split systems* are better known via phylogenetics, as in the book by Steel [36], and in recent papers by Catanzaro, Gambette, Balvočiūtė, Bryant, and Spillner [6, 22, 2]. Devadoss and Petti [11] showed that the space of circular split systems is an intuitive extension of the Billera-Holmes-Vogtmann space of phylogenetic trees [3], exhibiting a natural projection into the compactification of the real moduli space of curves [8, 9]. It is studied as a simplicial complex by Terhorst [37], and is related to the BME polytope and STSP polytope by Devadoss, Forcey, Scalzi, and Durell [10, 13, 16].

In our previous works [11, 15, 14], we study the space of circular split systems and a unique correspondence between these and circular electrical networks. We review these results in Section 2. We describe convenient maps between circular electrical networks and circular split systems in Section 3. The latter are simpler combinatorial structures well-studied in the field of phylogenetics, so our maps can be seen as invariants of the electrical networks. Section 4 introduces compactified split systems and extends the correspondence to electrical cactus networks. In particular, our graphical map ξ takes *any* compactified circular network (cactus network, planar or not) to a compactified *planar* split system. Our main result follows, a summary of Theorems 8 and 13 in Section 4:

Theorem 1. *For a planar cactus network N , the map ξ coincides with both the Kalmanson ρ and the induced σ split systems of the planar dual N^* . That is, $\xi(N) = \rho(N^*) = \sigma(N^*)$ and $\xi'(N^*) = \rho(N) = \sigma(N)$.*

Moreover, if the network N itself is planar, then $\xi(N)$ gives a shortcut to the alternative, well-known ways to find the associated split system via the Kalmanson map. Indeed, we show that the split systems in the image of this multi-named map have a particular form, known as *faithful* [15] — those systems which are made up of splits displayed by some network. These faithful systems are an important subcomplex of the space of circular systems.

Finally, Section 5 proves enumeration results (summarized by Table 1, page 22) across the spectrum of spaces and maps between them (showcased by Figure 6, page 12). Theorem 1 has an immediate application for counting the faithful split systems, resulting in the following (expanding Corollary 22) :

Corollary 2. *The number of cells in the complex of faithful split systems with n boundary nodes is*

$$\frac{1}{n+1} \left(\sum_{j_0+\dots+j_n=n} \left(\prod_{i=0}^n \left(\sum_{s \in \mathcal{P}_{j_i}} 2^{t(s)} \right) \right) \right),$$

where j_0, \dots, j_n are ordered non-negative integers, \mathcal{P}_{j_i} is the set of Ptolemy diagrams (from [26]) with j_i vertices, and $t(s)$ is the number of optional edges of s .

We obtain this by observing that including the induced system of a network with multiple connected components requires extension to the compactification of the space of systems, and vice versa: the induced systems with multiple components arise from cactus networks in the compactification of the space of electrical networks. This presents a challenge to our counting methods, but our new graphical maps solve the problem by undoing that switch: they preserve both the connected components and the cactus structure.

2. CLASSICAL SPACES

2.1. Circular Electrical Networks. Physically, a network N is made of conducting Ohmic wires with n exposed terminals that can be tested in order: We apply unit voltage to each of the terminals in turn while grounding all the remaining $n-1$ terminals. This defines the *response matrix* $M(N)$, recording the current at terminal j of N when the voltage is applied to terminal i as entry M_{ij} . Indeed, two circular electrical networks are *electrically equivalent* if they have the same response matrix. An equivalence class is planar if any representative is planar. The Kron reduction $K(N)$ is an invariant of the equivalence class of N , and several other invariants are discussed in [7].

A *circular electrical network* is a graph with a selected set of n *terminals* (or *boundary nodes*) labeled by $[n]$ and arranged on a circle. The rest of the graph lies inside the circle, and the *interior nodes* are unlabeled. The edges are weighted with positive real numbers which typically stand for the conductance of each connection. A *circular planar electrical network* N is one that can be represented with its terminals on a bounding circle and with no crossed edges in the disk. Usually the terminals are assumed to be numbered in clockwise order, and throughout this paper planarity is with respect to that order.¹

Figure 1(a) shows an example of a circular planar network N , where the non-labeled edges have conductance 1. This is a running example, and we show how to calculate the rest of Figure 1 in the following sections. The dual N^* shown in part (d) is calculated in Figure 5. The conductances of the Kron reduction of the dual are given by the off-diagonal entries of the response matrix $M(N^*)$, where

$$M(N^*) = \begin{bmatrix} -23/14 & 11/28 & 0 & 0 & 1/28 & 3/14 & 0 & 1 \\ 11/28 & -183/56 & 1 & 1 & 19/56 & 15/28 & 0 & 0 \\ 0 & 1 & -1 & 0 & 0 & 0 & 0 & 0 \\ 0 & 1 & 0 & -1 & 0 & 0 & 0 & 0 \\ 1/28 & 19/56 & 0 & 0 & -39/56 & 9/28 & 0 & 0 \\ 3/14 & 15/28 & 0 & 0 & 9/28 & -29/14 & 1 & 0 \\ 0 & 0 & 0 & 0 & 0 & 1 & -2 & 1 \\ 1 & 0 & 0 & 0 & 0 & 0 & 1 & -2 \end{bmatrix}$$

More practically, we could use an ohmmeter to test the resistance (impedance) between pairs of our terminals. We record these results as the *resistance matrix* $W(N)$, where W_{ij} is the effective resistance between i and j . The entries W_{ij} are a metric on the terminal nodes, as shown in [32]. Figure 2(a) shows a nonplanar case. Here are $M(N)$ and $W(N)$ for Figure 2(a):

$$M = \begin{bmatrix} -9/5 & 1/5 & 3/5 & 0 & 1 \\ 1/5 & -2 & 3/5 & 2/5 & 4/5 \\ 3/5 & 3/5 & -6/5 & 0 & 0 \\ 0 & 2/5 & 0 & -4/5 & 2/5 \\ 1 & 4/5 & 0 & 2/5 & -11/5 \end{bmatrix} \quad W = \begin{bmatrix} 0 & 1 & 13/12 & 31/16 & 3/4 \\ 1 & 0 & 13/12 & 23/16 & 3/4 \\ 13/12 & 13/12 & 0 & 109/48 & 4/3 \\ 31/16 & 23/16 & 109/48 & 0 & 23/16 \\ 3/4 & 3/4 & 4/3 & 23/16 & 0 \end{bmatrix}$$

Definition 3. For a circular electrical network N , its Kron reduction $K(N)$ is an equivalent network with the same terminal nodes as N , but no internal nodes. Two terminal nodes are directly connected by an edge in $K(N)$ if there is a path in N connecting them which does not go through other terminal nodes. An edge $\{i, j\}$ of $K(N)$ is given the weight $M_{ij}(N)$.

¹We will consider planarity with respect to any circular order in a future work.

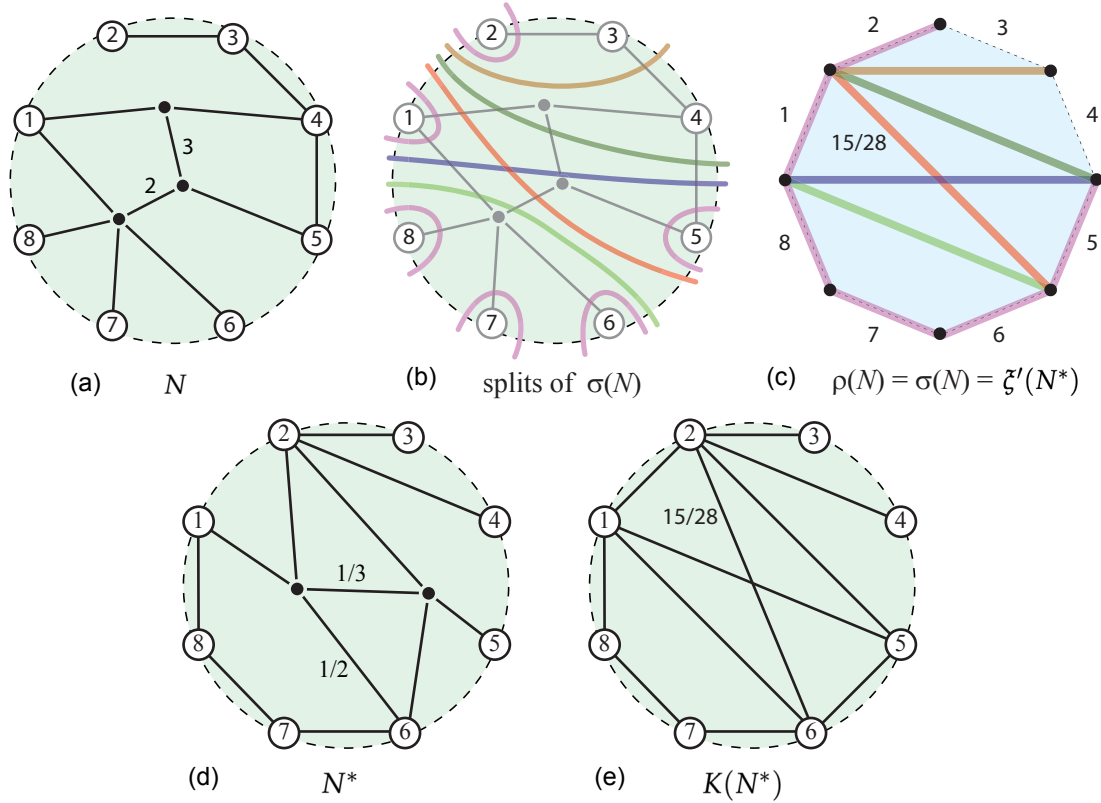


FIGURE 1. A planar network and the related structures that we will calculate. Top row shows (a) a clockwise planar electrical network N (with conductance 1 for non-labeled edges), (b) its splits $\sigma(N)$, (c) the polygon diagram of $\xi'(N^*) = \rho(N) = \sigma(N)$, (d) the dual N^* , and (e) the Kron reduction $K(N^*)$.

Figure 2(b) displays the Kron reduction for the network in part (a). Note that N and $K(N)$ have the same response matrix, and are therefore equivalent as circular electrical networks. In fact, the response matrix $M(N)$ is the Laplacian of the Kron reduction $K(N)$, and thus $K(N)$ can be viewed as a visualization associated with $M(N)$. Curtis and Morrow [7] defined a space of response matrices Ω_n as follows:

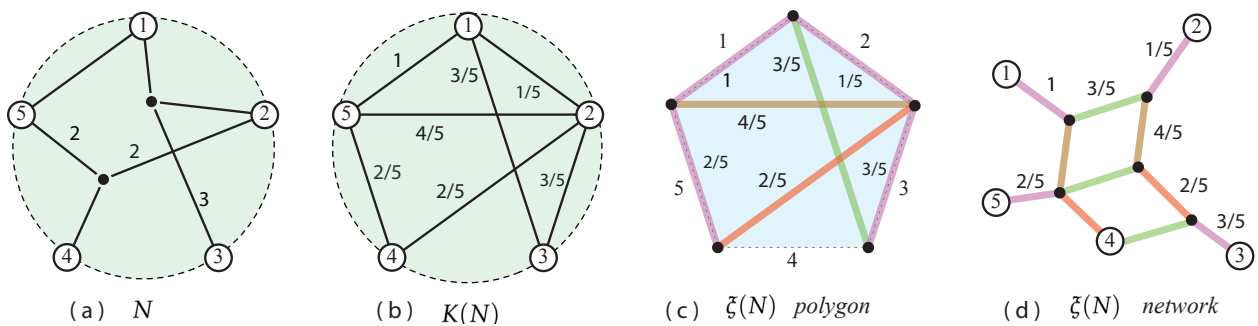


FIGURE 2. (a) A nonplanar (with respect to the clockwise order) circular electrical network N , (b) its Kron reduction $K(N)$, and graphical split system $\xi(N)$ in (c) polygonal and (d) split network formats.

Definition 4. Let Ω_n be the space of all response matrices for circular planar networks with n distinct boundary nodes, labeled by $[n]$ in clockwise order.

The space Ω_n is stratified into cells as a CW-complex. We use the same notation for the space and the face poset of cells.² For instance the enumeration of these cells $a_n = |\Omega_n|$ is given recursively by

$$(2.1) \quad a_n = 2(n-1)a_{n-1} + \sum_{j=2}^{n-2} (j-1)a_j a_{n-j}, \quad \text{where } a_0 = a_1 = 1, a_2 = 2.$$

This formula is shown in [1] and gives the OEIS sequence [A111088]. Each cell of dimension k in Ω_n corresponds to an (unweighted) electrical equivalence class of networks, and can be minimally represented by choosing conductance weights for a planar non-unique *critical* (or *reduced*) network with k edges. A cell x is contained in another cell y when the network corresponding to x can be found by either deleting or contracting edges of y . The left side of Figure 3 shows critical networks for each of the 52 cells of Ω_4 . Each column corresponds to cells of Ω_4 of a fixed dimension with f -vector $\langle 1, 6, 14, 16, 10, 4, 1 \rangle$.

2.2. Phylogenetic Split Systems. A *split* of $[n]$ is a bipartition $A|B$ of $[n]$ and a *split system* is any collection of splits of $[n]$. A graph with some of its nodes labeled by $[n]$ *displays* a split $A|B$ if there is a set of edges whose removal increases the number of connected components by one, and the two new components include respectively the nodes labeled by A and B . A *minimal display* of the split is a displaying set of edges that do not contain a proper subset displaying that split. A *split network* is a representation of a split system as a graph, where each split is minimally displayed by a set of parallel edges of the same length. A *circular split system* can be drawn with the n boundary nodes on the boundary of a disk, with non-crossing sets of parallel edges. The following space appears as a chamber in a larger theory of networks and trees in [11]:

Definition 5. Let Ψ_n be the space of weighted circular split systems on n boundary nodes, using the clockwise circular ordering of $[n]$.

The space Ψ_n is stratified with cells corresponding to split systems with no edge weighting. The total number of cells is $|\Psi_n| = 2^{\binom{n}{2}}$. A cell x is contained in another cell y when the system corresponding to x can be found by removing splits of y . In fact, as a CW-complex Ψ_n is equivalent to a positive orthant of $\mathbb{R}^{\binom{n}{2}}$. The right side of Figure 3 shows the cells of Ψ_4 , each column corresponds to cells of a fixed dimension, with f -vector $\langle 1, 6, 15, 20, 15, 6, 1 \rangle$, the 6th row of Pascal's triangle.

Remark. A circular split system can also be represented by a polygonal diagram [11]: the n terminals label the edges of an n -gon in some circular order, and each split is drawn as a diagonal. Figure 2 displays a polygonal diagram in (c) of the circular split system drawing in (d).

To any circular split system n , we can associate a *dissimilarity matrix*, an $n \times n$ real, symmetric, nonnegative matrix, where the (ij) -entry is the sum of the weighted splits between nodes i and j in

²The poset of cells is denoted EP_n in [1]

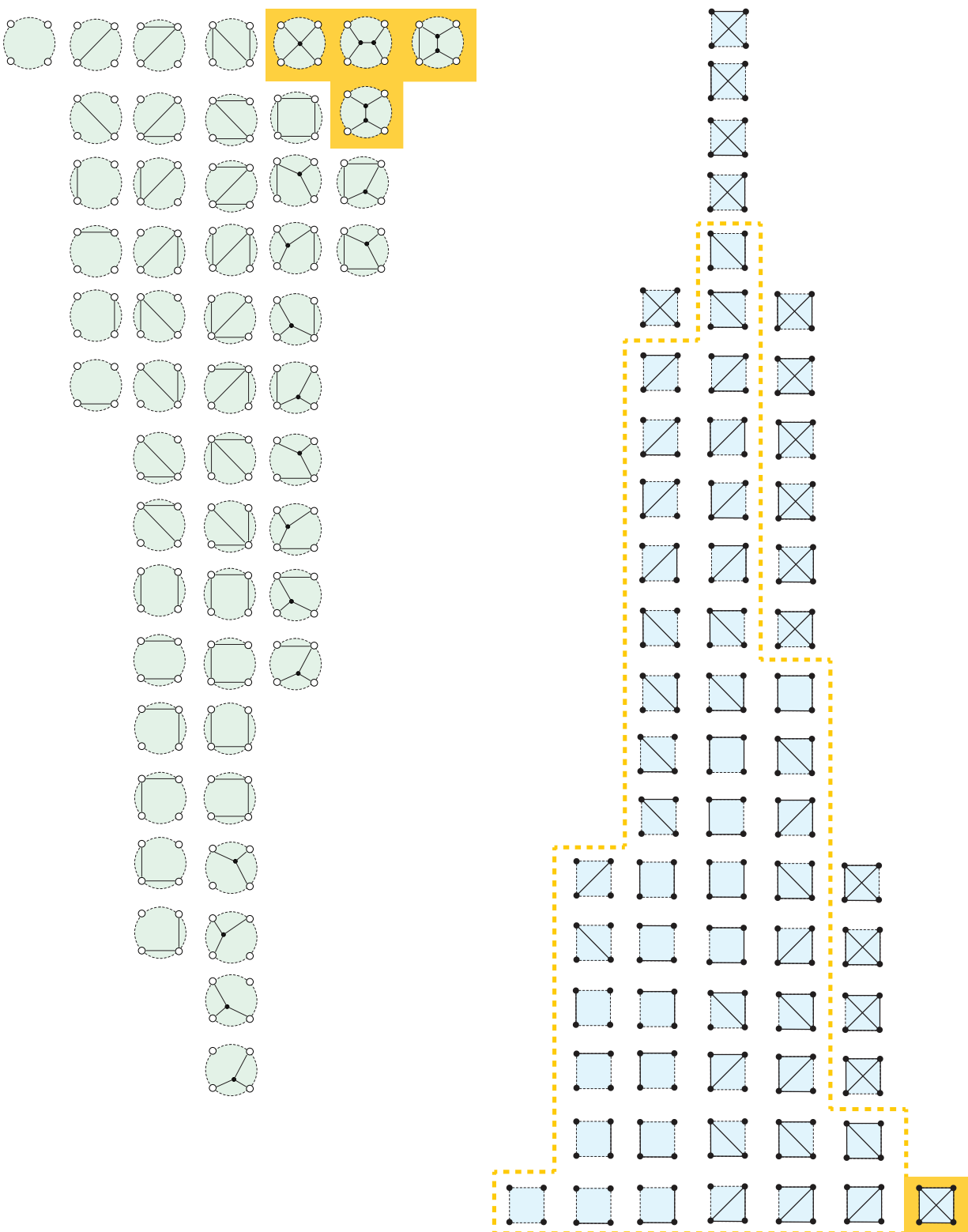


FIGURE 3. Combinatorial action of ξ on the cells of the space Ω_4 to Ψ_4 .

the network. In our case, the dissimilarity matrix is the resistance matrix W . It is well-known [36] that there is a bijection between weighted circular split systems and dissimilarity matrices satisfying the *Kalmanson condition*: there exists a circular order of the boundary such that for any four nodes i, j, k, l listed in that circular order,

$$\max(W_{ij} + W_{kl}, W_{jk} + W_{il}) \leq W_{ik} + W_{jl}.$$

Kalmanson proved that the metrics obeying this condition yield solutions to the Traveling Salesman Problem in polynomial time [27]. Thus, for a fixed circular labeling, the space of Kalmanson dissimilarity matrices of circular split systems on this labeling can be identified with Ψ_n .

3. MAPS BETWEEN CLASSICAL SPACES

3.1. Graphical Map ξ . We define a key function which takes any equivalence class of circular electrical networks as input and returns a circular *planar* split system. The input circular networks (and their response matrices) must be with respect to a given circular ordering, typically the clockwise order. While all our maps are defined on weighted networks (edges weighted with conductance and output weighted split systems), we often do abuse notation and apply the maps to unweighted input and output to see their purely combinatorial function.

Definition 6. *The graphical split system $\xi(N)$ of an electrical network N is the weighted circular planar split system constructed by putting the n boundary nodes of N in circular clockwise order and reinterpreting the Kron reduction network $K(N)$ as a polygon — shifting its terminals by a half-step counterclockwise rotation and labeling the exterior sides instead. The cographical split system $\xi'(N)$ for a circular electrical network N is similar but constructed with a half-step clockwise rotation.*

Here, each edge of $K(N)$ is reinterpreted as a split whose weight is equal to the conductance of the edge of $K(N)$. Since any response matrix M is seen as a Kron reduction, it is clear that ξ is injective and surjective, and a homeomorphism to the space of circular split systems with clockwise ordering. Indeed on the response matrices, it is just the identity map together with alternate interpretation of the effective conductance between node i and j , or upper-triangular (off-diagonal) entry $M_{i,j}$.³ Note that this immediately gives rise to a Kalmanson metric \mathbf{d}_ξ on $[n]$, where the distance $\mathbf{d}_\xi(i, j)$ between i and j is the sum of the splits that separate i from j .

Remark. *Interestingly, while this metric is the effective resistance $W(N^*)$ for the dual electric network N^* for circular planar networks N , no measurable interpretation of the metric \mathbf{d}_ξ exists in general.*

Figure 2 shows the process for ξ , starting with N and ending with a new circular split system $\xi(N)$. We show it in two forms, the easily seen polygonal picture in part (c) and a split network representation in part (d). Another case showing the combinatorial interpretation of ξ' is seen via the running example in Figure 1, where Figure 5 displays the dual network.

³For instance, if $n = 8$, $M_{3,8}$ is the weight of the split $\{4, 5, 6, 7, 8\}|\{1, 2, 3\}$.

Corollary 7. *The combinatorial map ξ respects the cell structure of Ω_n . That is, if $x \leq y$ for cells of Ω_n , then $\xi(x) \leq \xi(y)$.*

Proof. Deleting or contracting an edge of a minimal network x in Ω_n can only decrease or leave constant the number of edges in the Kron reduction, that is, the splits of $\xi(x)$. \square

Thus the action of ξ on the space of all electrical networks (all response matrices, using clockwise order) is an injective map which is surjective onto the space Ψ_n of circular planar split systems in clockwise order. However the action of ξ on the cell structure of Ω_n is an embedding into the cell structure of Ψ_n . Figure 3 shows the combinatorial action of ξ on the cells of the space Ω_4 . The map ξ takes all four networks (highlighted region at the top) to the single (highlighted region at the bottom) top-dimensional cell of Ψ_4 . The split systems not inside the dashed lines are not in the image of ξ .

3.2. Kalmanson Map ρ . Results in [14] and [15] introduced the correspondence between circular planar electrical networks and circular split systems. The latter paper proved the case for level-1 networks and the former for all connected circular planar electrical networks. Here, we extend that to the case of multiple connected components:

Theorem 8. *If a symmetric matrix M is a response matrix $M = M(N)$ for a circular planar electrical network N , then its resistance matrix $W(N)$ obeys the Kalmanson condition.*

Proof. The case for connected networks can be proven using either Kirchhoff and Ohm's laws [14] or Kenyon and Wilson's equation [29, Theorem 2.9]. The latter equation also applies to the disconnected case, where the resistance matrix will have zeros, which correspond to nodes with no split between them. \square

Theorem 8 implies that for any circular planar electrical network, there is a corresponding circular split system. The construction of that system is via the Buneman algorithm [36] or the Neighbor-Net algorithm [5]. The former requires precise resistances, but the latter can work with approximates. For accurate data, they both give the same result, which we define as follows:

Definition 9. *The Kalmanson split system $\rho(N)$ is the circular split system corresponding (injectively) to the (equivalence class of) circular planar electrical network N .⁴*

The Kalmanson map ρ can be extended to all (non-planar) electrical networks by letting even non-Kalmanson resistance metrics be subjected to the best-fit approximation of Neighbor-net. In that extension, the map will no longer be injective. Note also that the algorithm will find a circular order for which $W(N)$ is Kalmanson if possible. This output will only have the original circular order if the original is circular planar in that order.

⁴The Kalmanson map we call ρ here is just the extension of the map R_w defined in [14], from connected planar networks to all planar networks.

3.3. **Induced Map σ .** For the case of a connected circular planar electrical network as input, we define the induced split system.⁵ For a circular planar electrical network N , a *grove* is a spanning forest of the graph of N whose component trees each include some of the nodes labeled by $[n]$. A k -*grove* is a grove with k trees. The weight of a grove is the product of the weights of all the edges in that grove. A 2-grove of N *respects* a split that is minimally displayed by N if the two trees of the grove span the two components of the displayed split.

Definition 10. *The weight of a split displayed by a connected circular planar network N is the sum of the weights of 2-groves that respect it, divided by the summed weights of the spanning trees of N . The induced split system $\sigma(N)$ is the set of weighted splits displayed by N .*⁶

Theorem 11. *When restricted to circular planar electrical networks N , the induced split system coincides with the Kalmanson split system. That is, $\rho(N) = \sigma(N)$.*

Proof. We prove this for the case of a connected network N . For a network with more than one connected component, the proof applies to each separate component, via block-decomposition of the matrices. Consider a connected circular planar electrical network N which displays the splits $\sigma(N)$. Each split corresponds to a collection of the 2-groves that Kenyon and Wilson use in their formula for the resistance R_{ij} : the 2-groves that are possible after deleting any set of edges that display the split [29, Proposition 2.7]. Note that this correspondence partitions the 2-groves. Thus the sum of weights of the splits between two nodes is the same as the sum of the weights of the 2-groves. \square

Example. *The weight calculation is illustrated in Figure 4 for one of the splits of $\sigma(N)$ from Figure 1(b). There are 15 spanning trees of N and their weights sum to 56. For the split $\{1, 6, 7, 8\}|\{2, 3, 4, 5\}$, the figure shows the four ways to minimally display it, and beneath each we sum the weights of the 2-groves. The weights total to 30, and therefore the weight of the split is $30/56 = 15/28$. That value matches the conductance of the edge from 2 to 6 in $K(N^*)$, as shown in Figure 1.*

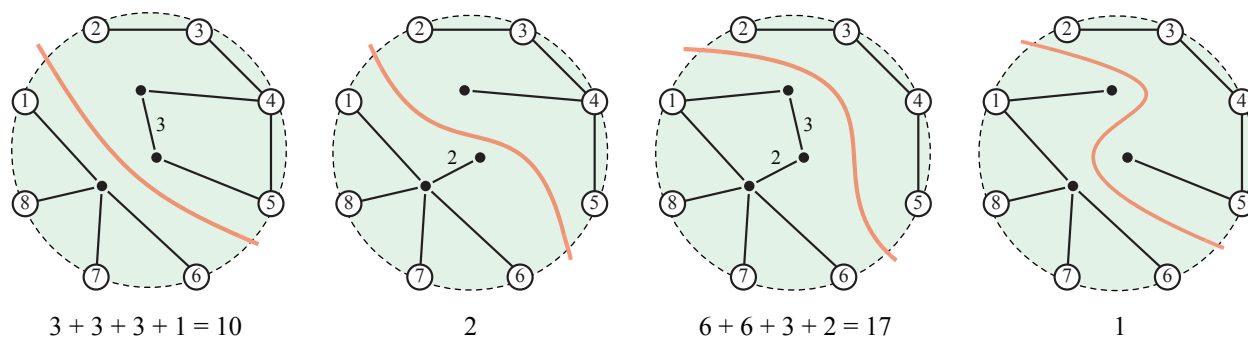


FIGURE 4. The weight calculation for one of the splits of $\sigma(N)$ from Figure 1(b).

⁵For electrical networks with multiple connected components, we must wait until we define the proper codomain — the compactification of the space of split systems — in Section 4.

⁶Our $\sigma(N)$ has the same (unweighted) split network as the map $\Sigma(N)$ from Gambette [16, 22].

3.4. Matchings and Duals. We construct the *dual* N^* of a planar circular electrical network N using *strand matchings*.⁷ We begin by constructing the *medial graph* of N . Each original edge of N becomes a new node, and any two new nodes arising from adjacent original edges of N are connected by a new edge of the medial graph. Original nodes at the boundary of N are always encircled by one of these new edges; and if the boundary node is degree one then the new edge will be a loop. However, we truncate the medial graph by deleting the portions that extend outside the boundary of N , leaving instead a pair of new nodes called *stubs* on either side of each original boundary node.

The *strand diagram* of N is found by tracing paths (called *strands*) in the medial graph, one starting from each stub, and turning neither left nor right at new nodes, but taking the straight option to arrive eventually at another stub. A *perfect matching* P on $[2n]$ is a set of n pairs $\{a, b\}$ where each element of $[2n]$ is used once. Every circular planar electrical network N gives rise to a perfect matching on $[2n]$, by following its strands. However, this matching depends on N and is not an invariant of the electrical equivalence class. To get an invariant matching, we need to restrict to the critical (reduced) representatives of that class [33].

To form the dual N^* we shift each original node of N counterclockwise on the boundary just past the stub on that side. It helps visually to shade the strand diagram in a checkerboard fashion, with original nodes in shaded regions. Figure 5 continues the example N from Figure 1(a) along with its strand diagram $P(N)$. After shifting the boundary nodes counterclockwise, they will be in unshaded regions. Now reverse the shading and put new interior nodes in the newly shaded interior regions. Edges connect any two nodes in adjacent regions via the intersection points of the strands to complete the picture of N^* . The perfect matching of $P(N)$ in Figure 5 has, for instance, pairs $\{1, 8\}$ and $\{2, 10\}$ while that of $P(N^*)$ has pairs $\{2, 9\}$ and $\{3, 11\}$.

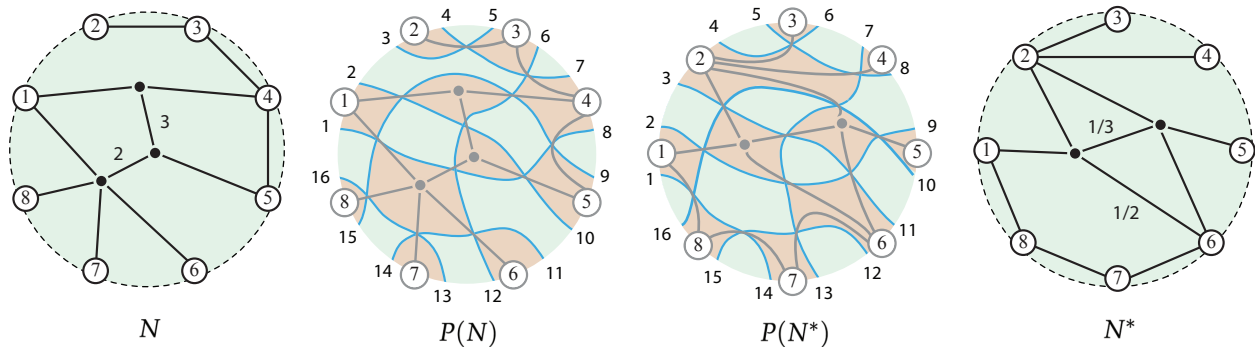


FIGURE 5. A circular planar electrical network N from Figure 1 and the construction of its planar dual N^* through strand diagrams.

Definition 12. For a circular planar electrical network N , the planar dual N^* is the network that corresponds to the same strand diagram $P(N)$ but with opposite shading. Each edge of N^* thus bisects an edge of N , where we assign the reciprocal of the edge weight to the bisecting edge of N^* .

⁷Another alternative replaces each edge with a perpendicular edge; this method is more difficult to extend to the compactified cactus networks, however.

Although the graphical map at first seems merely a visual coincidence, the next theorem shows that it actually extends our earlier maps to all circular networks, planar *and* nonplanar. Thus it exhibits all circular electrical networks (up to equivalence) in a one-to-one correspondence with all circular planar split systems, with the planar circular electrical networks embedded as a special subset.

Theorem 13. *When restricted to connected circular planar electrical networks N with a circular clockwise order of $[n]$, the graphical map ξ coincides with both the Kalmanson and the induced split systems of the planar dual. That is, $\xi(N) = \rho(N^*) = \sigma(N^*)$. Respectively, we have $\xi'(N^*) = \rho(N) = \sigma(N)$.*

Again we prove this for the case of a connected network N . For a network N with more than one connected component, the response matrix will decompose into blocks on the diagonal for each component. The resistance between components would be infinite, so mapping must be done component-wise, where the function ρ (finding the resistance W and the corresponding splits) can be applied for each component via its block matrix.⁸

Proof of Theorem 13. We choose to prove the version with $\xi'(N^*)$ as it is illustrated in Figure 1. The second equation $\rho(N) = \sigma(N)$ follows from Theorem 11. For the first equation, we relate $\xi'(N^*)$ and $\sigma(N)$. Each split in $\sigma(N)$ corresponds to the existence of at least one interior path in N^* . Thus each split corresponds to an edge in the Kron reduction of N^* , and so a split in $\xi'(N^*)$. The weight of the edge in the Kron reduction is the same as the weight of that split, since the edge in the Kron reduction gives the effective conductance using all the interior paths. \square

3.5. Summary of Maps. Figure 6 displays an overview all the maps discussed so far. We note that maps ξ and ξ' take as input any electrical network (regardless of planarity) and return a circular planar split system. However, these two maps rely on a given circular order of the boundary nodes, typically given as the clockwise order. In contrast, the map σ must take as input a circular planar electrical network N , and yet gives the same result if applied to an equivalent network with a different circular order. Finally, the map ρ takes as input any electrical network N — Kalmanson, planar, or neither, allowing for imperfect data — and returns a circular planar split system. However this output is only guaranteed to have resistances corresponding to the original network in the case that N has a Kalmanson resistance metric.

This construction raises new questions. First, although here we restrict our study to planar networks with a given clockwise order of nodes, the map ξ can operate on any network, as long as the nodes are given a clockwise order first. The results of that mapping for non-planar examples are interesting, but not studied here. Moreover, the general relationship between the weights of splits to their original conductances remains unknown.

Secondly the map ξ carries the structure of duality on electrical networks to a new duality on their image in the circular split systems. We note that the map ξ is reminiscent of the T -duality map on decorated permutations [34]. Moreover, ξ carries an equivalence relationship on circular split systems —

⁸For a network with more than one connected component, the split system we obtain will have multiple components, lying in the compactification of Ψ_n ; see Section 4.

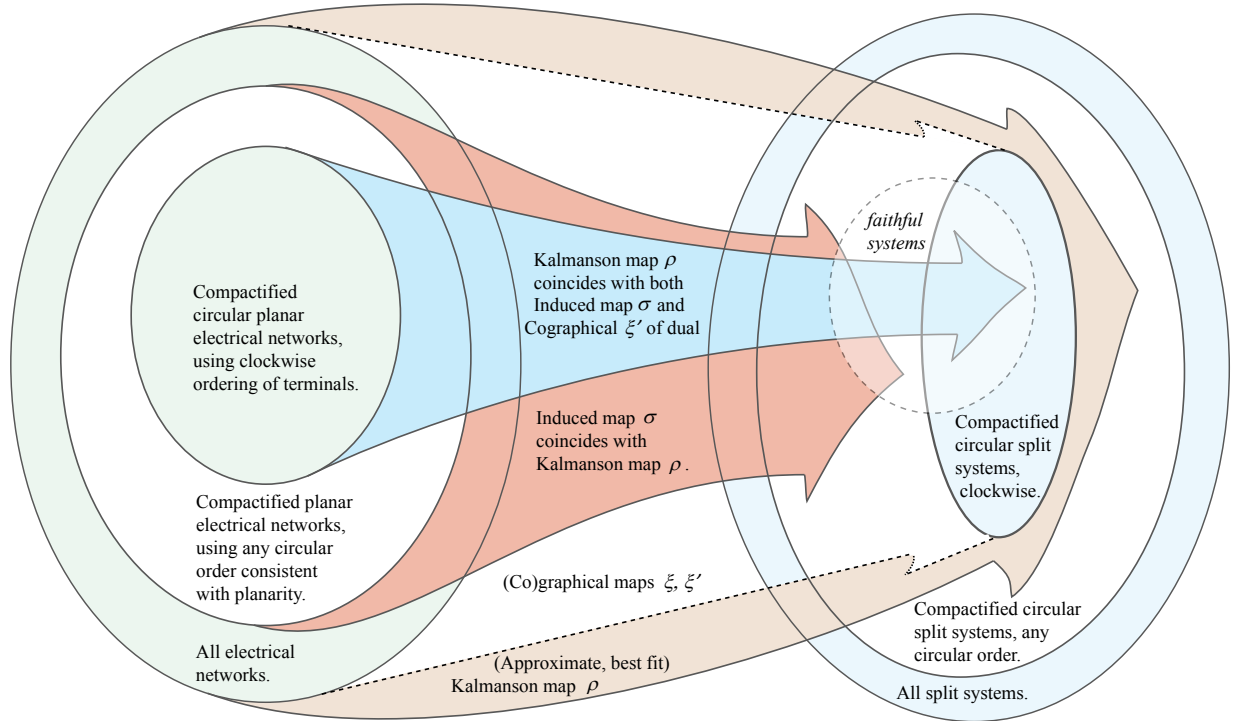


FIGURE 6. Domains and ranges for the maps in this paper.

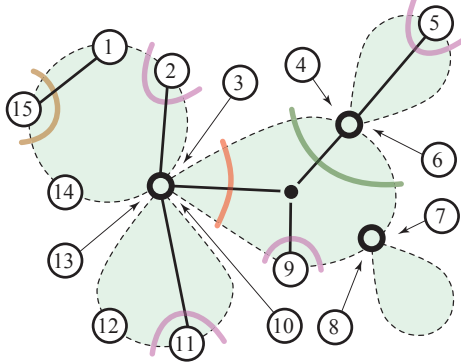
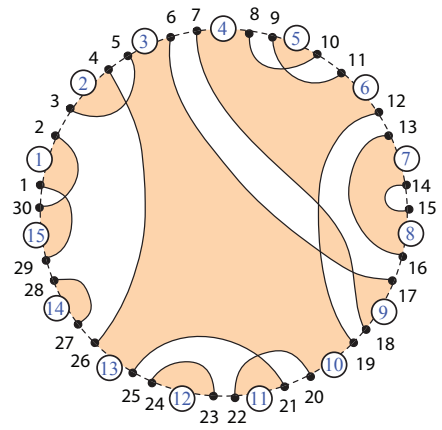
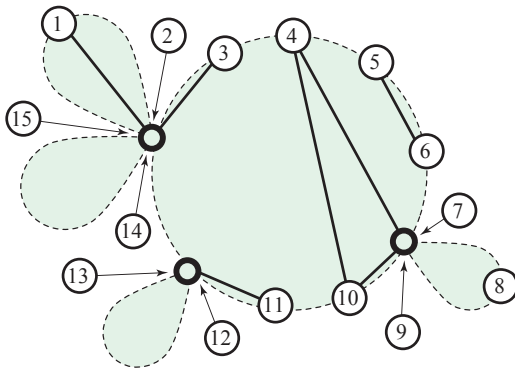
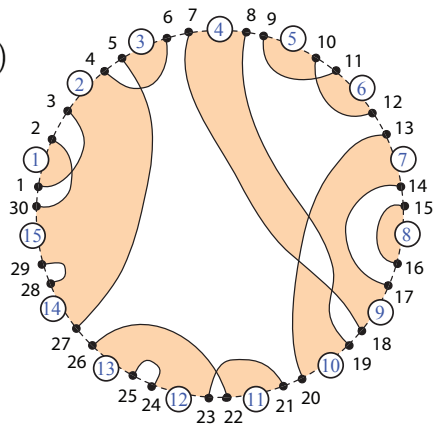
under twisting as defined by Devadoss and Petti [11] — to a new combinatorial equivalence on response matrices which rewires the (possibly nonplanar) electrical networks. What is the physical meaning of this equivalence? Indeed, ξ shows the poset and CW cell structures on circular split systems as a coarsening of those on circular planar networks. It also carries the cell structure of split systems to a new cell structure on all circular electrical networks. This new combinatorial structure is unexplored.

Remark. *Noting that a circular planar electrical network can have several consistent circular orders raises the question of a larger space of networks with any circular order allowed. We save the study of such spaces for future work.*

4. CACTUS NETWORKS AND COMPACTIFICATIONS

4.1. Cactii. A printed electrical circuit is made of conductors in a network, with terminal nodes on the exterior available for connections. Some of those exterior nodes are identical, short-circuited together so that they are interchangeable in terms of their use. Similarly, monozygotic twins can be seen as genetically the same for the purpose of reconstructing a family tree from the DNA samples of living individuals. On a larger scale, basic DNA sequences of extant individuals from a biologically diverse ecosystem can be equated when the species match. From our perspective, allowing nodes to be infinitely close to each other corresponds to compactifying spaces. Here we define and relate the compactification of phylogenetic split systems (from the DNA examples) to the well-studied compactification of circular electrical network space.

A *cactus electrical network* is a generalized circular planar network where boundary nodes are allowed to be identified. In particular, the *space of cactus networks* is the compactification of the space of circular planar networks: the conductance between two boundary nodes is allowed to become ∞ (thereby “short-circuiting” them). Figure 7(a) shows an example along with its set of splits, a construction described in [24, 33]. The cactus network N has an associated strand diagram $P(N)$ in part (b), which now can have several boundary nodes occupying the same shaded region. Again we use the medial graph of N . However, to draw the strands, place all the nodes in clockwise order on a single circular boundary. Include semi-circular strands around any disconnected boundary node, and require that any set of boundary nodes all occupying the same shaded region are a set identified in the network; see part (c). Just as in Definition 12, the strand diagram allows the construction of the planar dual N^* for a cactus network seen in Figure 7(d).

 (a) N

 (b) $P(N)$

 (d) N^*

 (c) $P(N^*)$

 FIGURE 7. Cactus network N , strand diagrams, and its dual N^* .

Two cactus networks are equivalent if they have the same response matrix. Lam [33] shows that the (unweighted) electrical equivalence classes of circular planar electrical networks, including those formed by identifying terminal points, correspond bijectively to the perfect matchings on $[2n]$. To find the perfect matching guaranteed by this bijection, the equivalence class must be represented by a reduced N . In that case, the strands of the strand diagram will obey the requirement that any two of them cross each other at most once.

Definition 14. For a given circular order on $[n]$, the space of equivalence classes of cactus networks is the compactification \mathfrak{Q}_n of the space of circular electrical networks Ω_n .⁹

The equivalence classes of unweighted cactus networks correspond to cells of a CW-complex structure on the space. (We abuse notation by denoting this face poset as \mathfrak{Q}_n as well.) Cell containment is seen by deletion or contraction of any edges.

Example. Figure 8(a) illustrates the complex of unweighted equivalence classes of cactus networks for $n = 3$. Since the face poset \mathfrak{Q}_n is isomorphic to the poset P_n of perfect matchings, $|\mathfrak{Q}_n| = (2n - 1)!!$.

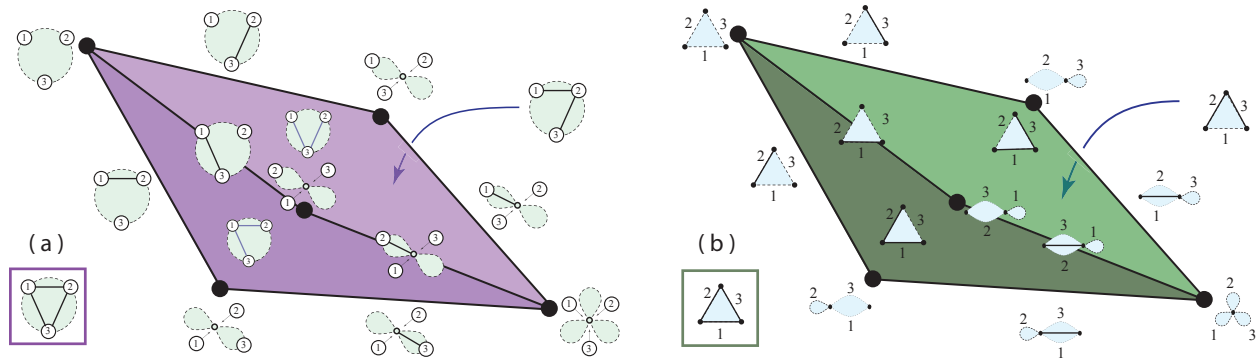


FIGURE 8. The graphical map ξ from cactus networks \mathfrak{Q}_3 to compactified split systems \mathfrak{P}_3

4.2. Compactifying Split Systems. Trees are a special case of both circular electrical networks and split systems. Kim [31] introduced a compactification by allowing edges of trees to become infinite in weight, resulting in a space of “phylogenetic oranges” [35]. Since resistance of ∞ corresponds to conductance of 0, the compactification of split systems will correspond to cactus networks.

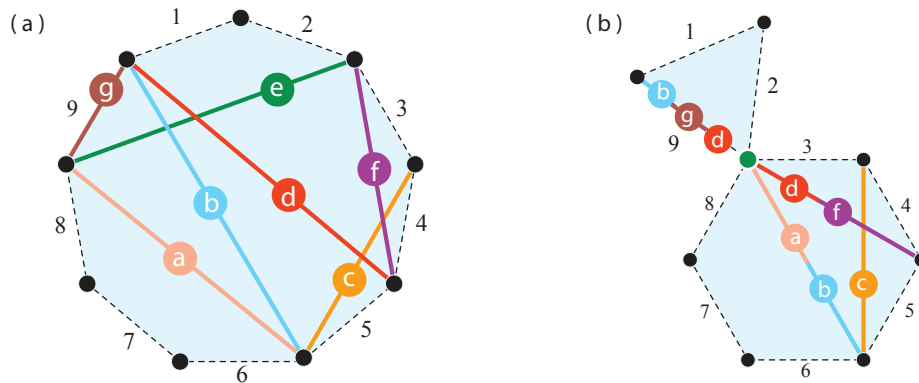


FIGURE 9. Compactifying by weighting edge e to become ∞ .

An analogous procedure can be followed for weighted split systems. Consider the dual polygon representation of a system in Figure 9(a). When we compactify this network by allowing an edge (say

⁹In [33], the space \mathfrak{Q}_n is denoted as E_n .

the diagonal ‘ e ’ labeled in green) to become infinite in weight, this corresponds to contracting the edge to a vertex, where the ends of any edges intersecting e are also contracted along with e ; see part (b). Note that this is dual to identification in cactus networks since resistance is the reciprocal of conductance. If this contraction results in overlapping of edges, the weights of these edges are summed. This is observed for edges $g + b + d$ in Figure 9(a) as well as $a + b$ and $d + f$ in part (b).

Thus, a *compactified split system* for a given circular order of $[n]$ is a *noncrossing partition* on $[n]$ and a weighted split system on each part of that partition. Figure 10 shows the associated compactified split system to the network N^* from Figure 7, with splits appropriately color-coded.

Definition 15. *The space Ψ_n is the set of weighted compactified circular split systems with circular order $[n]$. It is the set of Kalmanson metrics making up the blocks of $n \times n$ dissimilarity matrices W .*

The unweighted compactified split systems on $[n]$ correspond to the cells of a CW-complex structure on Ψ_n . Containment of cells corresponds to either deletion or contraction (via infinity) of splits. The dimension of the top-dimensional cells of Ψ_n is $\binom{n}{2}$, since that is the maximum number of splits compatible with a single circular order.

Example. *Figure 8(b) shows the CW-complex structure of the space Ψ_3 , whereas Figure 11 shows the 1-skeleton of Ψ_4 : vertices in blue, edges in red. The f -vector for Ψ_4 is $(14, 28, 29, 24, 15, 6, 1)$ with 117 total cells. The 0-cells are counted by the Catalan numbers, since they correspond to the non-crossing partitions. Formulas for the total numbers of cells are given by Theorem 17 and its corollaries.*

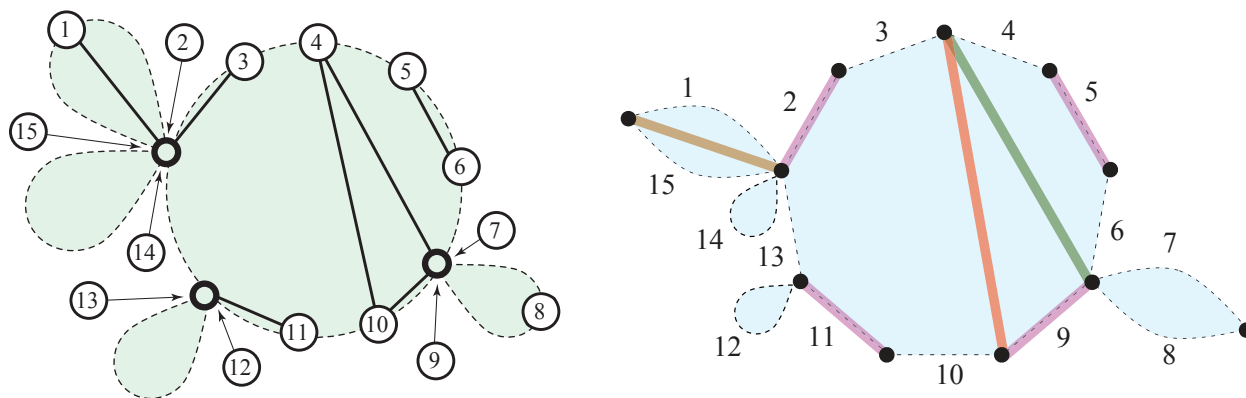
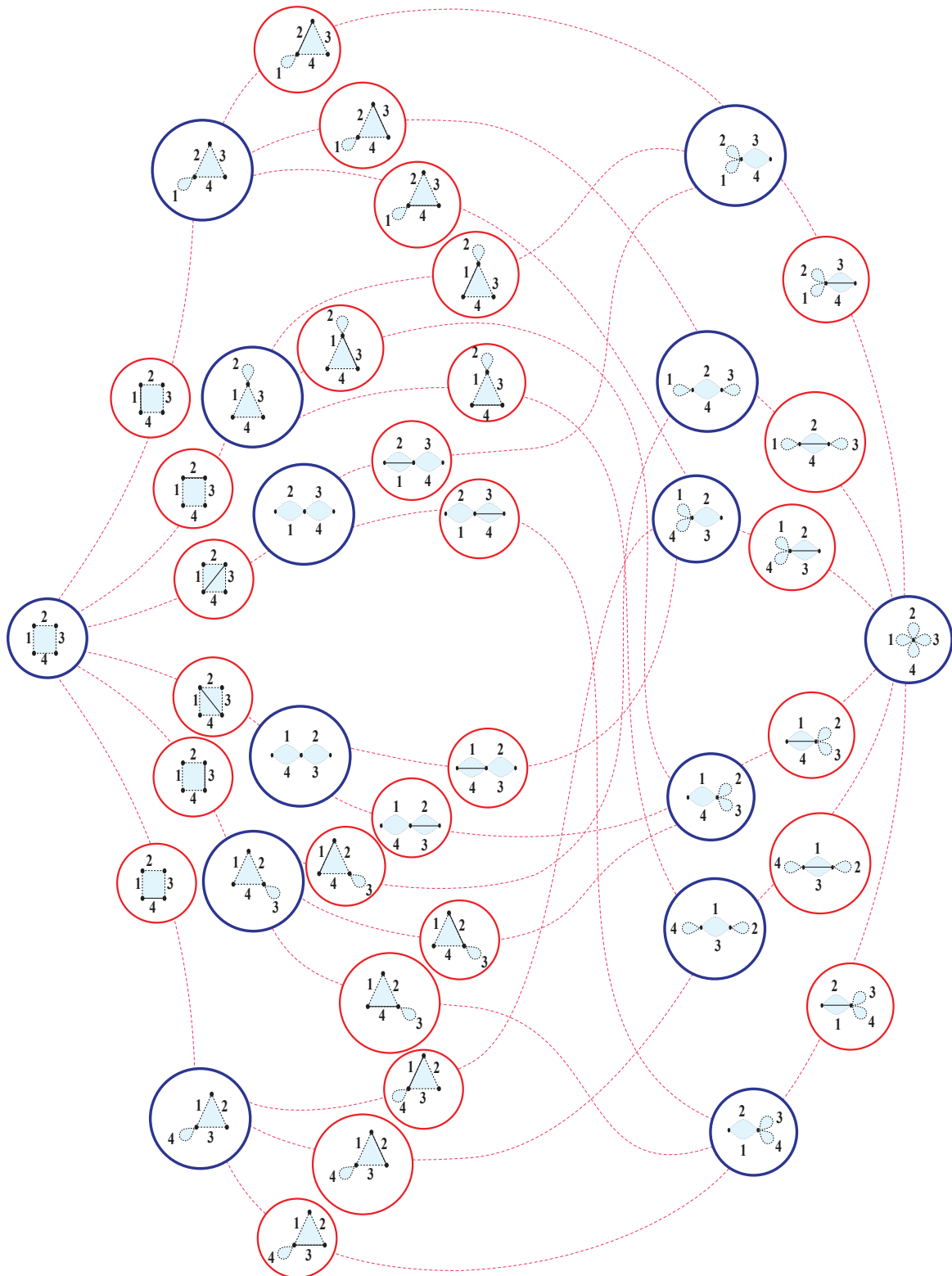


FIGURE 10. The compactified split system $\sigma(N) = \xi'(N^*)$ associated to the network from Figure 7.

4.3. Maps. We extend the maps defined in Section 3 to take cactus networks as input. The process is largely straightforward, but we need to carefully define the Kron reduction and response/resistance matrices of a cactus network in order to see the operation of ξ and ρ .

The Kron reduction $K(N)$ of a cactus network can be performed one bulb at a time, or expanded in a disk to show edges with infinite conductance. This expansion allows the edges of $K(N)$ to correspond to the entries in the response matrix $M(N)$. Note that when there is an edge of N incident on a

FIGURE 11. The 1-skeleton of Ψ_4 .

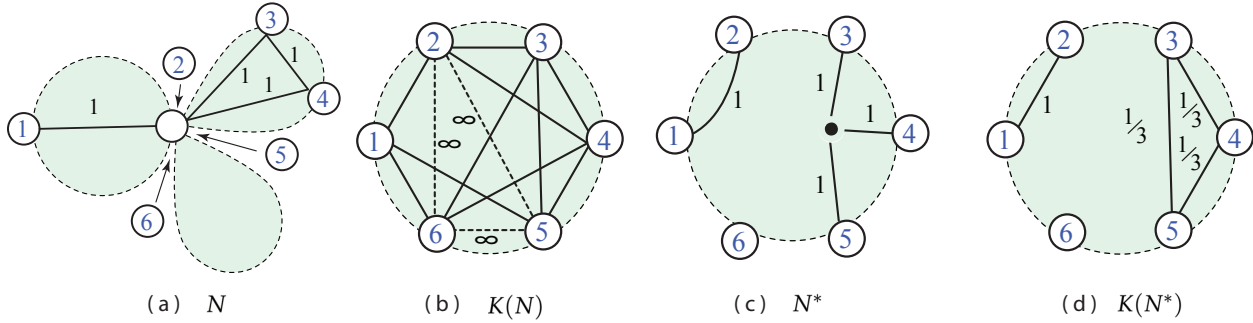


FIGURE 12. Cactus networks, duals, and Kron reductions.

(compactified) vertex (with multiple labels), the edges in $K(N)$ — and thus the entries in $M(N)$ — must evenly divide that conductance. Moreover, the response matrix of a cactus network will have entries of ∞ for the conductance between nodes that share a vertex, and corresponding diagonal entries of $-\infty$. The resistance matrix will have entries of 0 for pairs of nodes that share a vertex of the cactus network, but the other entries can be calculated directly by isolating the two nodes and using Kirchoff and Ohm's laws to find effective resistance between them.

Example. Figure 12 shows a cactus network N and its dual N^* together with their Kron reductions and split systems. For instance the edge from 1 to the vertex labeled 2,5,6 has conductance 1; therefore the edges $\{1, 2\}$, $\{1, 5\}$, $\{1, 6\}$ all have conductance $1/3$ in $K(N)$ as seen in the response matrix here:

$$M(N) = \begin{bmatrix} -1 & 1/3 & 0 & 0 & 1/3 & 1/3 \\ 1/3 & -\infty & 1/3 & 1/3 & \infty & \infty \\ 0 & 1/3 & -2 & 1 & 1/3 & 1/3 \\ 0 & 1/3 & 1 & -2 & 1/3 & 1/3 \\ 1/3 & \infty & 1/3 & 1/3 & -\infty & \infty \\ 1/3 & \infty & 1/3 & 1/3 & \infty & -\infty \end{bmatrix} \quad W(N) = \begin{bmatrix} 0 & 1 & 5/3 & 5/3 & 1 & 1 \\ 1 & 0 & 2/3 & 2/3 & 0 & 0 \\ 5/3 & 2/3 & 0 & 2/3 & 2/3 & 2/3 \\ 5/3 & 2/3 & 2/3 & 0 & 2/3 & 2/3 \\ 1 & 0 & 2/3 & 2/3 & 0 & 0 \\ 1 & 0 & 2/3 & 2/3 & 0 & 0 \end{bmatrix}$$

$$M(N^*) = \begin{bmatrix} -1 & 1 & 0 & 0 & 0 & 0 \\ 1 & -1 & 0 & 0 & 0 & 0 \\ 0 & 0 & -2/3 & 1/3 & 1/3 & 0 \\ 0 & 0 & 1/3 & -2/3 & 1/3 & 0 \\ 0 & 0 & 1/3 & 1/3 & -2/3 & 0 \\ 0 & 0 & 0 & 0 & 0 & 0 \end{bmatrix} \quad W(N^*) = \begin{bmatrix} 0 & 1 & \infty & \infty & \infty & \infty \\ 1 & 0 & \infty & \infty & \infty & \infty \\ \infty & \infty & 0 & 2 & 2 & \infty \\ \infty & \infty & 2 & 0 & 2 & \infty \\ \infty & \infty & 2 & 2 & 0 & \infty \\ \infty & \infty & \infty & \infty & \infty & 0 \end{bmatrix}$$

The extension of the induced map σ gives us the ability to define it for inputs N of both cactus networks and cactus networks with multiple connected components: We simply treat each connected component of N separately. The connected components of N give us a partition of $[n]$ with parts the boundary nodes of each component; this is the partition for $\sigma(N)$. The splits of $\sigma(N)$ on each part are those displayed in that component, with weights calculated via the spanning trees and 2-groves of that component using the edge weights (conductances).¹⁰ We get the following:

¹⁰The multiple labels on nodes make no difference to the weight of a grove.

Theorem 16. *For cactus network N , the map ξ coincides with both the Kalmanson and the induced split systems of the planar dual. That is, $\xi(N) = \rho(N^*) = \sigma(N^*)$. Respectively, we have $\rho(N) = \sigma(N) = \xi'(N^*)$.*

Proof. A cactus network N has bulbs separated by vertices which are the boundary nodes sharing several labels from $[n]$. No dual edge can connect nodes from separate bulbs. Thus the dual N^* has connected components that correspond to the bulbs of N . Vice-versa, connected components of N correspond to bulbs in the dual N^* .

First then, the mapping of combinatorial structure can be treated just as for the single-bulb (ordinary) circular planar electrical networks, one bulb of the cactus network at a time. The same is true for electrical networks with more than one connected component: each component can be seen to contribute its own collection of splits on its own boundary nodes. For N a cactus network, the response of the (disconnected) dual network $M(N^*)$ will decompose into blocks on the diagonal, one for each bulb of N , with other entries zero. The resistance matrix $W(N^*)$ will have corresponding blocks of the same size but with other entries ∞ . The maps $\xi'(N^*)$ and $\rho(N^*)$ can thus operate block-wise.

To see that this block-wise operation gives the expected values of the weights of the splits, we note that the process of compactifying a split system (via treating some splits as infinite) sums the weights of the splits which coincide after collapsing infinite edges to a point; see Figure 9. Thus the weight of the final split in the compactified system $\xi(N)$ is the same as the edge in the Kron reduction of a single bulb, which is the weight of the split found by $\rho(N^*)$ as in the connected case (Theorem 13). \square

5. ENUMERATION

5.1. Lagrange Inversion. Our graphical map ξ takes any compactified circular network to a compactified planar split system. We leverage this map and show how to count these systems, all based on the following result:

Theorem 17. *For a given circular order on $[n]$, the number of unweighted compactified split systems is given by the OEIS sequence A136654. The generating function is given by*

$$A(x) = \left(\frac{1}{x}\right) \text{Inverse} \left(\frac{x}{B(x)}\right), \quad \text{where } B(x) = \sum_{k=0}^{\infty} 2^{\binom{k}{2}} x^k,$$

and “Inverse” refers to taking the inverse function.

Remark. *To find the number of compactified split systems on n , use the Lagrange inversion theorem on $x/B(x)$: Find the series expansion for $(B_n(x))^{n+1}$ (where $B_n(x)$ is the partial series up to x^n), take the coefficient of x^n in that expansion, and divide by $n+1$. For instance, when $n=4$, we see*

$$(1 + x + 2x^2 + 8x^3 + 64x^4)^5 = 1 + 5x + 20x^2 + 90x^3 + 585x^4 + O(x^5),$$

where $585/5 = 117$, the coefficient of x^4 (585) divided by $n+1$ (5) results in the fourth term (117) of sequence A136654.

Proof. We start by associating a species A to the combinatorial structures of compactified split systems. Define $A([n])$ to be the set of pairs made up of a compactified split system on $[n]$ and a permutation on $[n]$. The permutation can be thought of as a 1-1 mapping of the exterior labels in their cyclic order to a new set of numerical tags $\{1, \dots, n\}$. This allows us to consider $A(x)$ as simultaneously the ordinary generating function of the numbers of structure (types) of compactified split systems and the exponential generating function of the species A .

Next, any instance of this species on $[n]$ can be created with the following steps. First we choose k tags: any subset of $[n]$ of size k , and also a subset S_1 of our original cyclic labels of size k but required to contain the label 1.¹¹ The tags are attached to the labels in S_1 (in any order) and a set of splits is assigned to S_1 . There are $2^{\binom{k}{2}}$ possibilities for those splits.

Set S_1 is a part of a noncrossing partition of the circular labels $[n]$, and the remaining labels not in S_1 are subdivided by the contiguous portions of S_1 into at most k contiguous (in the circular order) sets. These sets are then used to continue the process: the species A is applied to each of them recursively, with all the possible partitions of the remaining $n - k$ tags. Thus we see a functional equation for the species:

$$A = \sum_{k=0}^{\infty} 2^{\binom{k}{2}} X^k A^k,$$

or equivalently, $A = B \circ (X \cdot A)$. Then in terms of exponential generating functions, $A(x) = B(xA(x))$. Multiplying both sides by x and rearranging yields

$$x = \frac{x A(x)}{B(x A(x))},$$

which implies

$$x A(x) = \text{Inverse} \left(\frac{x}{B(x)} \right)$$

and thus our result. □

5.2. Corollaries. The following is an immediate consequence:

Corollary 18. *Counting the compactified split systems for a given circular order on $[n]$ yields*

$$|\mathbb{P}_n| = \frac{1}{n+1} \left(\sum_{j_0 + \dots + j_n = n} \left(\prod_{i=0}^n 2^{\binom{j_i}{2}} \right) \right),$$

where the sum is over ordered lists of non-negative integers summing to n .

For comparison, the numbers of unweighted equivalence classes of cactus networks for a given circular order are given by $(2n - 1)!!$, which counts the perfect matchings on $[2n]$. For instance, for a given circular order of $[4]$, there are 15 compactified split systems not corresponding to a cactus network — they correspond instead to non-planar cactus networks. At the same time, there are 4 types of unweighted planar cactus networks on $[4]$ that all map to the same split system: the top dimensional

¹¹For instance, to make the structure in Figure 10 we let $k = 2$ and chose $S_1 = \{1, 15\}$. The tags are not shown in Figure 10 because we only wanted to display the structure type.

cell plus 3 more planar cactus networks whose Kron reduction is the complete graph, as seen in Figure 3. Thus the counts of cells compare: $117 - 15 + 3 = 105$.

Moreover, we can also count the compactified electrical networks, using the same arguments as in the proof of Theorem 17, or via a comment of P. Hanna in entry [A111088] of [?]:

Corollary 19. *Counting the compactified electrical networks yields*

$$|\mathfrak{Q}_n| = \frac{1}{n+1} \left(\sum_{j_0+\dots+j_n=n} \left(\prod_{i=0}^n |\mathfrak{Q}_{j_i}| \right) \right) = (2n-1)!! ,$$

where $|\mathfrak{Q}_n|$ is the number of distinct classes of non-compact electrical networks, by Equation (2.1).

5.3. Plabic Tilings and Ranges. Counting phylogenetic networks is an active area of research, with the application of bounding the search time for reconstruction algorithms [4, 23]. An especially useful sort of phylogenetic split system is the induced split system $\sigma(N)$, as described combinatorially by Gambette, Huber, and Scholz [22]. These are somewhat difficult to count, especially when we allow for multiple connected components, for two reasons. First, the induced split system for networks with multiple connected components is a compactified split system, as first defined in this paper. Second, the fact that the induced map takes disconnected networks to compact split systems, and compact networks to disconnected split systems, means that it is hard to count the split systems in its range using a recursive species procedure, at first glance.

However, our new graphical map ξ doesn't have that problem: it preserves the connected components and the compactified (cactus) structure, so we can enumerate the items in the range of ξ using our functional formula $A = B \circ (X \cdot A)$. Theorem 1 then tell us that the graphical map and the induced map have the same overall range, so by counting one you count the other. Thus the first step is to report a method for counting the non-compact image of ξ , so that we have input for our final count.

Definition 20. *For an n -node circular planar electrical network N , the plabic tiling $\tau(N)$ is a collection of polygons with edges labeled with $[n]$, each subdivided and shaded as follows: There is one polygon for each part of the partition making up the cographical split system $\xi'(N^*)$. Add any diagonal that is a bridge in $\xi'(N^*)$. Regions of $\xi'(N^*)$ with no diagonal edges are shaded in $\tau(N)$ whereas regions of $\tau(N)$ that correspond to complete graphs in $\xi'(N^*)$ remain unshaded.*

Example. *Figure 13 shows the construction of $\tau(N)$. We use $\xi'(N^*)$ from Figure 1, but note that the result is easy to see directly from observing the edges of $K(N^*)$.*

Curtis and Morrow [7] show that a planar circular electrical network gives rise to a response matrix M with non-negative circular minors. In particular, this means that for any pair of crossing diagonals in the Kron reduction, the four other diagonals using the endpoints of the two crossing diagonals must be present. That feature guarantees that the Kron reduction will appear as non-overlapping cliques and empty polygonal regions, which we state as the following:

Corollary 21. *If a circular electrical network N is planar, then the Kron reductions $K(N^*)$ and $K(N)$, and thus the split systems $\xi'(N^*)$ and $\xi(N)$, allow constructions of the plabic tilings $\tau(N^*)$ and $\tau(N)$.*

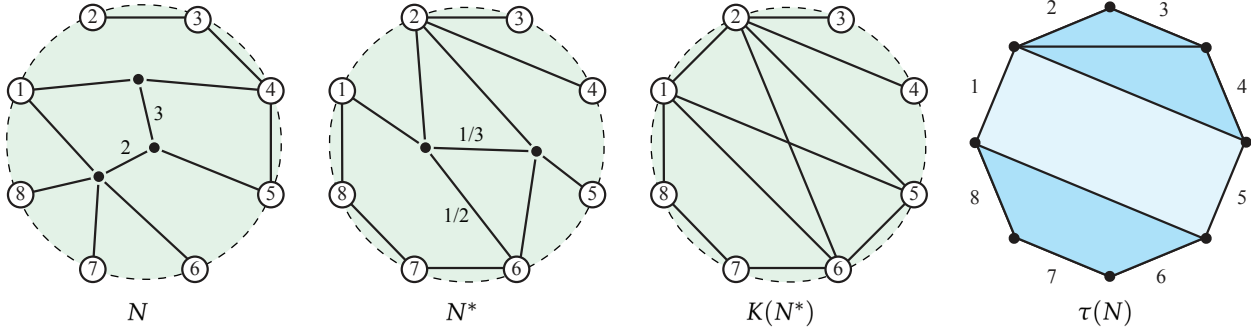


FIGURE 13. Networks from Figure 5 along with $K(N^*)$ and the plabic tiling $\tau(N)$.

This result points out that the construction of $\tau(N)$ is always possible when N is planar. Thus there are certain obstructions to planarity easily visible in the Kron reduction. Figure 14 shows two networks N' and N'' obtained by adding a wire to network N from Figure 1. The graph of $K(N')$ cannot be transformed to a plabic tiling, and therefore N' cannot be planar, from Corollary 21. On the other hand, N'' and $K(N'')$ show that the converse is not always true: there might be values of the conductances in N'' making the network planar.

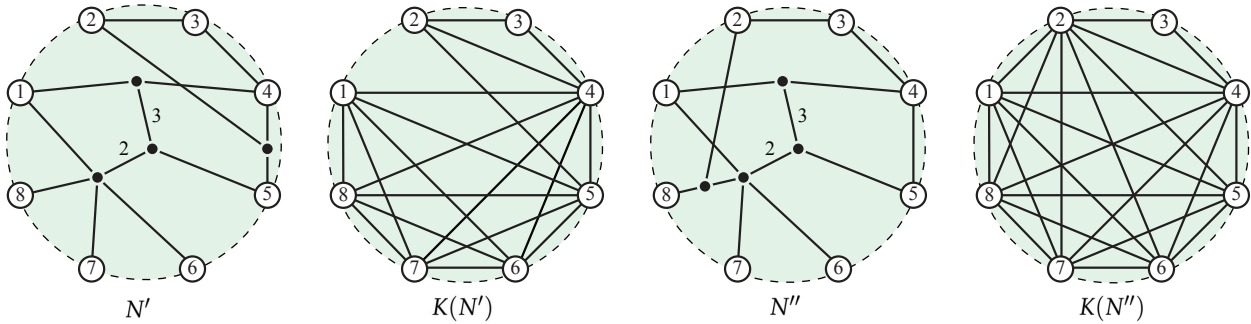


FIGURE 14. Altering a network N by adding a wire to get N' and N'' .

From Theorem 1, and noting that taking the dual is a bijective operation on the (clockwise ordered) compactified electrical networks \mathfrak{Q}_n , we conclude that the image of \mathfrak{Q}_n under ξ is the same as its image under σ . We call that image the *faithful* split systems as in [15]. Thus for compact clockwise networks, the faithful (unweighted) split systems (that is, the unweighted induced systems) are counted by $|\sigma(\mathfrak{Q}_n)| = |\xi(\mathfrak{Q}_n)|$. These cells form a subcomplex of Ψ_n . The f -vector of that subcomplex for $n = 4$ is $\langle 14, 28, 28, 20, 9, 2, 1 \rangle$.

The total number of (noncompact) unweighted split systems in the image $\xi(\mathfrak{Q}_n)$ in Ψ_n , which form a subcomplex of Ψ_n , can be counted using a formula found in [26]. There, the Ptolemy diagrams are described as polygons with a subset of diagonals, obeying the rule that for every pair of crossing diagonals in a diagram, all the other diagonals using their four endpoints (edges of a quadrilateral) must be included in that diagram.¹² This rule precisely describes the Kron reductions of circular planar

¹²The Ptolemy diagrams correspond to torsion pairs in the cluster category of type A_n [26].

n	$ \Omega_n $	$ \mathfrak{Q}_n $	$ \Psi_n $	$ \mathfrak{P}_n $	$ \xi(\Omega_n) $	$ \sigma(\mathfrak{Q}_n) = \xi(\mathfrak{Q}_n) $
1	1	1	1	1	1	1
2	2	3	2	3	2	3
3	8	15	8	15	8	15
4	52	105	64	117	49	102
5	464	945	1024	1565	373	839
OEIS	[A111088]	[A001147]	[A006125]	[A136654]	[?]	[?]

TABLE 1. Enumeration of cells in each CW complex.

electrical networks (in clockwise order), with the extra requirement that the boundary edges (between consecutive nodes on the boundary) all be included. The Ptolemy diagrams \mathcal{P}_n of the n -gon for $n = k+3$ are counted in [26] by

$$|\mathcal{P}_n| = \frac{1}{k+2} \sum_{j=0}^{\lfloor \frac{k+1}{2} \rfloor} 2^j \binom{k+1+j}{j} \binom{2k+2}{k+1-2j},$$

resulting in the OEIS sequence [A181517]. Note that the plabic tilings of a single polygon with n sides are in direct bijection with the Ptolemy diagrams of size n , for $n \geq 3$. We also include the unique diagrams of size $n = 2, 1$, and 0 : a single edge (a trivial split), a single vertex, and the empty diagram.

We wish to count the cells in the image $\xi(\Omega_n)$. The only difference between the polygonal pictures of split systems in the image of ξ and the Ptolemy diagrams is that the boundary edges (trivial splits) of the former can be included or excluded, when they are not part of a clique of size 4 or more. Denoting the number of these optional trivial splits for a given diagram s by $t(s)$ we have:

$$|\xi(\Omega_n)| = \sum_{s \in \mathcal{P}_n} 2^{t(s)}.$$

Example. When $n = 4$, the four Ptolemy diagrams are $Pt_4 = \{\boxtimes, \boxplus, \boxminus, \square\}$. Thus we have $|\xi(\Omega_4)| = 2^0 + 2^4 + 2^4 + 2^4 = 49$, as seen in Figure 3, inside the dashed line. For $n = 1, \dots, 6$ we have $|\xi(\Omega_n)| = 1, 2, 8, 49, 373, 3196$ respectively.

The proof of Theorem 17 can now be easily used to count the images of compactified electrical networks:

Corollary 22. *The enumeration of the images of compactified electrical networks yields*

$$|\xi(\mathfrak{Q}_n)| = |\sigma(\mathfrak{Q}_n)| = \frac{1}{n+1} \left(\sum_{j_0 + \dots + j_n = n} \left(\prod_{i=0}^n |\xi(\Omega_{j_i})| \right) \right).$$

Expanding this formula gives Corollary 2. For example, when $n = 4$, we have the total:

$(1/5)(5(49) + 20(8) + 10(4) + 30(2) + 5(1)) = 102$. A summary of early results is given by Table 1.

REFERENCES

- [1] Joshua Alman, Carl Lian, and Brandon Tran. Circular planar electrical networks: posets and positivity. *J. Combin. Theory Ser. A*, 132:58–101, 2015.
- [2] Monika Balvočiūtė, David Bryant, and Andreas Spillner. When can splits be drawn in the plane? *SIAM J. Discrete Math.*, 31(2):839–856, 2017.
- [3] L. Billera, S. Holmes, and K. Vogtmann. Geometry of the space of phylogenetic trees. *Adv. in Appl. Math.*, 27(4):733–767, 2001.
- [4] Mathilde Bouvel, Philippe Gambette, and Marefatollah Mansouri. Counting Phylogenetic Networks of level 1 and 2. *Journal of Mathematical Biology*, 81(6):1357–1395, 2020.
- [5] D. Bryant and V. Moulton. Neighbor-net: An agglomerative method for the construction of phylogenetic networks. *Molecular Biology and Evolution*, 21:255–265, 2004.
- [6] Daniele Catanzaro, Martin Frohn, Olivier Gascuel, and Raffaele Pesenti. A tutorial on the balanced minimum evolution problem. *European Journal of Operational Research*, 2021.
- [7] Edward B. Curtis and James A. Morrow. *Inverse Problems For Electrical Networks*. World Scientific, London, 2000.
- [8] Satyan L. Devadoss. Tessellations of moduli spaces and the mosaic operad. In *Homotopy invariant algebraic structures (Baltimore, MD, 1998)*, volume 239 of *Contemp. Math.*, pages 91–114. Amer. Math. Soc., Providence, RI, 1999.
- [9] Satyan L. Devadoss. Combinatorial equivalence of real moduli spaces. *Notices Amer. Math. Soc.*, 51(6):620–628, 2004.
- [10] Satyan L. Devadoss, Cassandra Durell, and Stefan Forcey. Split network polytopes and network spaces. *SLC 82B, Proceedings of FPSAC 31, to appear*, 2019.
- [11] Satyan L. Devadoss and Samantha Petti. A space of phylogenetic networks. *SIAM Journal on Applied Algebra and Geometry*, 1:683–705, 2017.
- [12] Florian Dörfler and Francesco Bullo. Kron reduction of graphs with applications to electrical networks. *IEEE Trans. Circuits Syst. I. Regul. Pap.*, 60(1):150–163, 2013.
- [13] Cassandra Durell and Stefan Forcey. Level-1 phylogenetic networks and their balanced minimum evolution polytopes. *J. Math. Biol.*, 80(5):1235–1263, 2020.
- [14] Stefan Forcey. Circular planar electrical networks, split systems, and phylogenetic networks. *SIAM Journal on Applied Algebra and Geometry*, 7(1):49–76, 2023.
- [15] Stefan Forcey and Drew Scalzo. Phylogenetic networks as circuits with resistance distance. *Frontiers in Genetics*, 11:1–17, 2020.
- [16] Stefan Forcey and Drew Scalzo. Galois connections for phylogenetic networks and their polytopes. *J. Algebraic Combin.*, 54(1):173–203, 2021.
- [17] Pavel Galashin. *Totally Positive Spaces: Topology and Applications*. ProQuest LLC, Ann Arbor, MI, 2019. Thesis (Ph.D.)—Massachusetts Institute of Technology.
- [18] Pavel Galashin, Steven N. Karp, and Thomas Lam. The totally nonnegative part of G/P is a ball. *Adv. Math.*, 351:614–620, 2019.
- [19] Pavel Galashin, Steven N. Karp, and Thomas Lam. Regularity theorem for totally nonnegative flag varieties. *Sém. Lothar. Combin.*, 84B:Art. 31, 12, 2020.
- [20] Pavel Galashin, Steven N. Karp, and Thomas Lam. The totally nonnegative Grassmannian is a ball. *Adv. Math.*, 397:Paper No. 108123, 23, 2022.
- [21] Pavel Galashin, Alexander Postnikov, and Lauren Williams. Higher secondary polytopes and regular plabic graphs. *arXiv 1909.05435*, 2019.
- [22] P. Gambette, K. T. Huber, and G. E. Scholz. Uprouted phylogenetic networks. *Bulletin of Mathematical Biology*, 79(9):2022–2048, Sep 2017.
- [23] Philippe Gambette, Katharina Huber, and Steven Kelk. On the challenge of reconstructing level-1 phylogenetic networks from triplets and clusters. *Journal of Mathematical Biology*, 74(7):1729–1751, 2017.
- [24] Yibo Gao, Thomas Lam, and Zixuan Xu. Electrical networks and the grove algebra. *arxiv.org*, 2022.
- [25] Patricia Hersh and Richard Kenyon. Shellability of face posets of electrical networks and the CW poset property. *Adv. in Appl. Math.*, 127:Paper No. 102178, 37, 2021.
- [26] Thorsten Holm, Peter Jørgensen, and Martin Rubey. Ptolemy diagrams and torsion pairs in the cluster category of Dynkin type A_n . *J. Algebraic Combin.*, 34(3):507–523, 2011.
- [27] Kenneth Kalmanson. Edgeconvex circuits and the traveling salesman problem. *Canadian J. Math.*, 27(5):1000–1010, 1975.
- [28] R. Kenyon. The Laplacian on planar graphs and graphs on surfaces. In *Current developments in mathematics, 2011*, pages 1–55. Int. Press, Somerville, MA, 2012.
- [29] Richard W. Kenyon and David B. Wilson. Boundary partitions in trees and dimers. *Trans. Amer. Math. Soc.*, 363(3):1325–1364, 2011.

- [30] Richard W. Kenyon and David B. Wilson. The space of circular planar electrical networks. *SIAM J. Discrete Math.*, 31(1):1–28, 2017.
- [31] J. Kim. Slicing hyperdimensional oranges: The geometry of phylogenetic estimation. *Molecular Phylogenetics and Evolution*, 17:58–75, 2000.
- [32] D. J. Klein and M. Randić. Resistance distance. *J. Math. Chem.*, 12(1-4):81–95, 1993.
- [33] Thomas Lam. Electroid varieties and a compactification of the space of electrical networks. *Adv. Math.*, 338:549–600, 2018.
- [34] Tomasz Lukowski, Matteo Parisi, and Lauren Williams. The positive tropical grassmannian, the hypersimplex, and the $m=2$ amplituhedron. *arxiv.org/abs/2002.06164*, 2020.
- [35] Vincent Moulton and Mike Steel. Peeling phylogenetic ‘oranges’. *Adv. in Appl. Math.*, 33(4):710–727, 2004.
- [36] Mike Steel. *Phylogeny—discrete and random processes in evolution*, volume 89 of *CBMS-NSF Regional Conference Series in Applied Mathematics*. Society for Industrial and Applied Mathematics (SIAM), Philadelphia, PA, 2016.
- [37] Jonathan Terhorst. The Kalmanson Complex. *arXiv*, 2011.

(S. Devadoss) UNIVERSITY OF SAN DIEGO, SAN DIEGO, CA 92110

Email address: devadoss@sandiego.edu

URL: satyandevadoss.org

(S. Forcey) UNIVERSITY OF AKRON, AKRON, OH 44325

Email address: sforcey@uakron.edu

URL: www.math.uakron.edu/~sf34